JGR Atmospheres

RESEARCH ARTICLE
10.1029/2026JD046823

Key Points:

- The frequency of extratropical cyclones is expected to decrease, but their minimum pressure and low-level winds are projected to intensify
- Future extreme cyclones tracks show reduced zonal pathways and an increase through the Southeast U.S. moving north along the coast
- Downscaling results project non monotonic yet increasingly intensified and broadened wind field changes from the present to late century

Supporting Information:

Supporting Information may be found in the online version of this article.

Correspondence to:

A. Ramos-Valle,
aramos@ucar.edu

Citation:

Ramos-Valle, A., Prein, A. F., Jaye, A., & Emanuel, K. (2026). Projected changes in wind hazards from extreme extratropical cyclones in the Northeastern U.S.. *Journal of Geophysical Research: Atmospheres*, *131*, e2026JD046823. https://doi.org/10.1029/2026JD046823

Received 2 MAR 2026
Accepted 24 AUG 2026

Author Contributions:

Conceptualization: Alexandra Ramos-Valle, Andreas F. Prein, Kerry Emanuel
Data curation: Abby Jaye
Formal analysis: Alexandra Ramos-Valle
Funding acquisition: Andreas F. Prein, Kerry Emanuel
Methodology: Alexandra Ramos-Valle
Project administration: Alexandra Ramos-Valle, Andreas F. Prein
Software: Alexandra Ramos-Valle, Andreas F. Prein, Abby Jaye
Visualization: Alexandra Ramos-Valle, Andreas F. Prein, Abby Jaye
Writing – original draft: Alexandra Ramos-Valle
Writing – review & editing: Alexandra Ramos-Valle, Andreas F. Prein, Abby Jaye, Kerry Emanuel

Projected Changes in Wind Hazards From Extreme Extratropical Cyclones in the Northeastern U.S.

Alexandra Ramos-Valle[1], Andreas F. Prein[1,2], Abby Jaye[1], and Kerry Emanuel[3]

[1]U.S National Science Foundation National Center for Atmospheric Research (NSF NCAR), Boulder, CO, USA, [2]Institute for Atmospheric and Climate Science, ETH Zurich, Zürich, Switzerland, [3]Massachusetts Institute of Technology, New Harbor, ME, USA

Abstract Extratropical Cyclones (ETCs) can produce high-impact weather in mid-latitudes, leading to extreme precipitation, winds, and storm surges. Despite the societal and economic impacts of ETCs, gaps remain in our understanding of how ETCs and their related hazards will change in a changing climate. In this study, we evaluate systematic changes in end-of-century ETC characteristics, including intensity, translation speed, and storm size, with a particular focus on evaluating how wind hazards related to ETCs are expected to change under future climate conditions. We leverage the 100-member Community Earth System Model 2 Large Ensemble (LENS2) data set to identify ETCs that traverse the Northeastern U.S. Results indicate that while the annual frequency of ETCs is projected to decrease under future climate conditions, the minimum pressure decreases and maximum low-level winds are projected to increase. We also observe track density changes in extreme future ETCs in the Northeast, with more frequent trajectories passing through the Southeastern U.S. and less zonal translation. Additionally, we leverage MPAS's variable-resolution capabilities to downscale a subset of extreme ETC events from LENS2 to a 3-km grid over the Northeast. Results highlight a shift toward more intense cyclones, with maximum 10 m and low-level wind speeds increasing by 28% between present and the end of the century.

Plain Language Summary Extratropical Cyclones (ETCs) are storms common in the mid-latitudes that produce high-impact events such as extreme precipitation, winds, and storm surge. Despite the societal and economic impacts of ETCs, there are gaps in our understanding of ETCs and how these will be different in the future. In this study, we thus study changes in ETC characteristics including their intensity, translation speed and storm size, with a focus on how wind hazards from ETCs are expected to change. Our study reveals that while the annual frequency of ETCs is projected to decrease under future climate conditions, they are expected to become more intense. We also observe track density changes in extreme future ETCs in the Northeast, with more frequent trajectories passing through the Southeastern U.S. and less zonal translation. Additionally, we leverage the variable resolution capabilities of model for prediction across scales to downscale a subset of extreme ETC events from LENS2 to 3-km grid spacing over the Northeast. Results highlight a shift to more intense cyclones, with maximum 10 m wind speeds and maximum low-level winds increasing by 28% from the current time period to the end of the century.

1. Introduction

Extratropical cyclones (ETCs) are important features in the atmospheric circulation in the mid-latitudes, producing high-impact weather including extreme winds, precipitation and flooding (Nederhoff et al., 2024; Sinclair et al., 2020). In the U.S., ETC events lead to significant socioeconomic losses, with direct impacts on the built environment and critical infrastructure. The northeastern U.S., characterized by highly populated urban areas and high-value properties and assets (Letson et al., 2021), is particularly vulnerable to ETC impacts. The top 10 windstorms during 1979–2018 over the northeastern states caused property damage losses of $24 million to $29 billion, with nine out of the 10 storms causing loss of lives (Letson et al., 2021). These significant impacts from ETCs in the northeastern U.S., particularly their potential for highly damaging winds, highlight the need to evaluate projected systematic changes in ETC characteristics. While there is a general consensus in the scientific literature suggesting that ETC frequency is expected to decrease in the future, uncertainty remains in projections of ETC intensity. The goal of this study is thus to improve our understanding of ETC wind risk in the Northeastern U.S., under current and future climate conditions.

10.1029/2026JD046823

We evaluate systematic changes in end-of-century ETC characteristics, including frequency, intensity, translation speed and storm size. We leverage the 100-member Community Earth System Model 2 (CESM2) Large Ensemble (LENS2) data set to identify ETCs that transect the Northeastern U.S., similar to methods in Karwat et al. (2024), Konstali et al. (2024) and Michalek (2024). Multiple identification and tracking algorithms have been developed, including methods by Murray and Simmonds and Murray (1991), Pinto et al. (2005), Blender et al. (1997), and Prein et al. (2023), all of which use mean sea level pressure as a proxy variable for cyclone detection. Previous studies have shown that while the annual number of ETCs is projected to decrease, storms with the highest near-surface wind speeds and lowest pressure anomalies are increasing under warmer conditions (Catto et al., 2019; Colle et al., 2015; Michaelis et al., 2017).

Additionally, we leverage the variable resolution capabilities of the Model for Prediction Across Scales (MPAS; Skamarock et al., 2014) to downscale extreme ETC events from LENS2 to 3-km grid spacing over the Northeast and evaluate changes in storm characteristics.

The article is organized as follows: In Section 2, we introduce the ERA5 and the CESM2-LE data, the MOAAP tracking algorithm and the methodology for analysis and dynamical downscaling with the MPAS model. In Section 3, we evaluate cyclone frequency and characteristics under recent and future climate conditions, and present results from extreme ETC events downscaled with MPAS. Finally, we discuss the conclusions of this study and potential applications in Section 4.

2. Data and Methods

2.1. CESM2 Large Ensemble

We identify ETCs in the CESM2 Large Ensemble (LENS2; Danabasoglu, Lamarque, et al., 2020; Rodgers et al., 2021) data set. LENS2 consists of 100 ensemble members at a 1° horizontal grid spacing. The simulations cover the period between 1850 and 2100 and use the historical (1850–2014) and future (2015–2100) SSP370 radiative forcing scenarios from CMIP6 (Eyring et al., 2016). Notably, 10 ensemble members in LENS2– referred to as the mother of all runs (MOAR)– contain a comprehensive set of high-frequency output fields (6-hr intervals) that can be used for downscaling experiments.

2.2. ERA5 Reanalysis

To assess the LENS2 model skill in simulating ETCs under recent climate conditions, we identified ETCs passing through the region of interest and compared the LENS2-derived climatology of frequency and intensity to that of ETCs tracked in the European Centre for Medium-Range Weather Forecasts reanalysis (ERA5; Hersbach et al., 2020) data set for the period 1940–2019, when data are mutually available. ERA5 data, available at a horizontal grid spacing of 0.25°, were regridded to 1° grid spacing.

2.3. Tracking and Evaluating Extratropical Cyclones

We tracked cyclones using the Multi-Object Analysis of Atmospheric Phenomena (MOAAP; Prein et al., 2023) tracking tool. MOAAP identifies ETCs by detecting sea level pressure (SLP; ≤ -8 hPa) and 500 hPa geopotential height anomalies (Z500; ≤ -80 m) that persist for more than 12 hr. To achieve this, MOAAP first applies a uniform square filter with a length of 100 km to the original fields, thus removing small-scale noise and local orographic effects. Then, the background environment in which cyclones exist is calculated by using a uniform square filter with a side length of 3,000 km and a temporal extent of 78 hr. Anomalies in SLP and Z500 are calculated by subtracting the background state from the smoothed fields. The resulting anomaly field is thresholded using the above-mentioned values, creating a binary mask field used for object identification. MOAAP then allows for the calculation of object characteristics such as area and center of mass.

We tracked cyclones globally but for this work, we focus on events impacting the U.S. Northeast coastal region (Figure 1), with particular attention to the region defined by a square area from 39°N to 45°N, and −68°W to −74°W, centered over Boston, MA (Figure 2).We tracked all ETCs in the 100 LENS2 member ensemble for the period 1850–2100 and evaluated them according to the following time periods: 1991–2020 (present); 2031–2060 (mid-century projections), and 2070–2099 (end-of-century projections). Intense ETC events in LENS for each time period were selected according to the maximum wind speed in the land area around Boston based on data from the first model level. We compared the ETC climatology derived from ERA5 and LENS2, including the

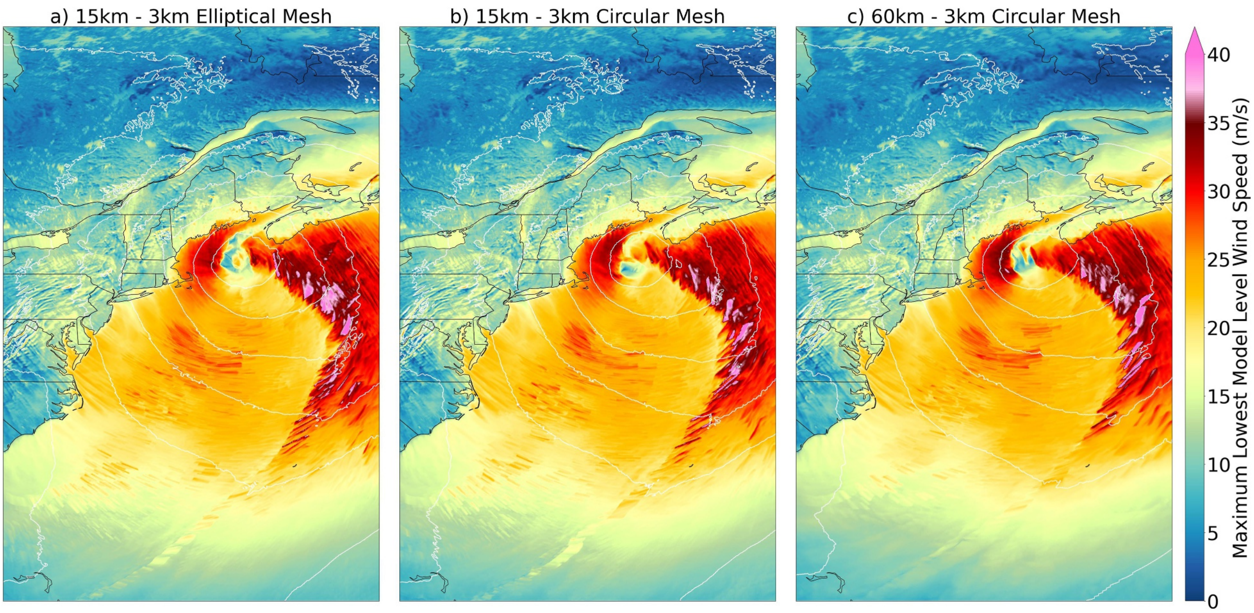

Figure 1. Example for testing different model for prediction across scales mesh configurations. Comparison of simulated maximum low-level wind speed at the same time step using the (a) 15–3 km elliptical, (b) 15–3 km circular and (c) 60–3 km circular meshes for the same test case.

ETC track density, and probability density functions for maximum wind speed, minimum pressure, translation speed, cyclone size and seasonal cyclone.

2.4. Downscaling With MPAS

ETCs were dynamically downscaled using the MPAS–Atmosphere version 8.0.1, a non-hydrostatic atmosphere model designed for weather and climate applications (Skamarock et al., 2012). Each MPAS simulation was initialized using atmospheric, land surface, and sea surface temperature states from the corresponding LENS2 member. To capture the storm's evolution, simulations were initialized 24 hr prior to the occurrence of peak wind speeds in the Boston area.

The parameterization schemes used to approximate subgrid-scale processes include the following: Thompson microphysics scheme (non-aerosol aware; Thompson et al., 2008), the Grell-Freitas (2014) convection, MYNN boundary layer scheme (Nakanishi & Niino, 2006; Olson et al., 2019) and surface layer (Olson et al., 2021) schemes, Rapid Radiative Transfer Model for General Circulation Models (RRTMG) for shortwave and long-wave radiation parameterization (Iacono et al., 2008), and the Noah land surface model (He et al., 2023). These schemes are used in the MPAS "convection_permitting" physics suite, which allows for both explicitly resolved hydrostatic and non-hydrostatic motions.

To select the most appropriate and efficient quasi-uniform and refined mesh, three variable resolution meshes were tested. Two 15–3 km variable resolution meshes were tested, where the global resolution is 15 km and the resolution was gradually reduced to 3 km over a refined area. The first mesh configuration had an elliptical refinement region that spanned approximately 60 degrees of latitude and 80 degrees of longitude. The second had a circular refinement region spanning approximately 60 degrees of latitude and longitude. The third and final mesh tested was a 60–3 km mesh with a circular 3 km refinement area of 16°. To test each of the mesh configurations, we downscaled three LENS2 ETCs in the period 1990–2020 according to maximum wind speed and three ETCs according to their minimum pressure, resulting in a total of nine test runs. Each ETC simulation was run for 3 days, with the MPAS run being initialized 24 hr before the time of maximum wind/minimum pressure identified in the LENS2 data. Output was saved at 1-hr intervals.

Based on comparisons of computation cost, runtime, output size and simulation results the 60–3 km MPAS grid was selected. This configuration represents a significant reduction in computation costs and minor differences between the outputs (Figure 1).

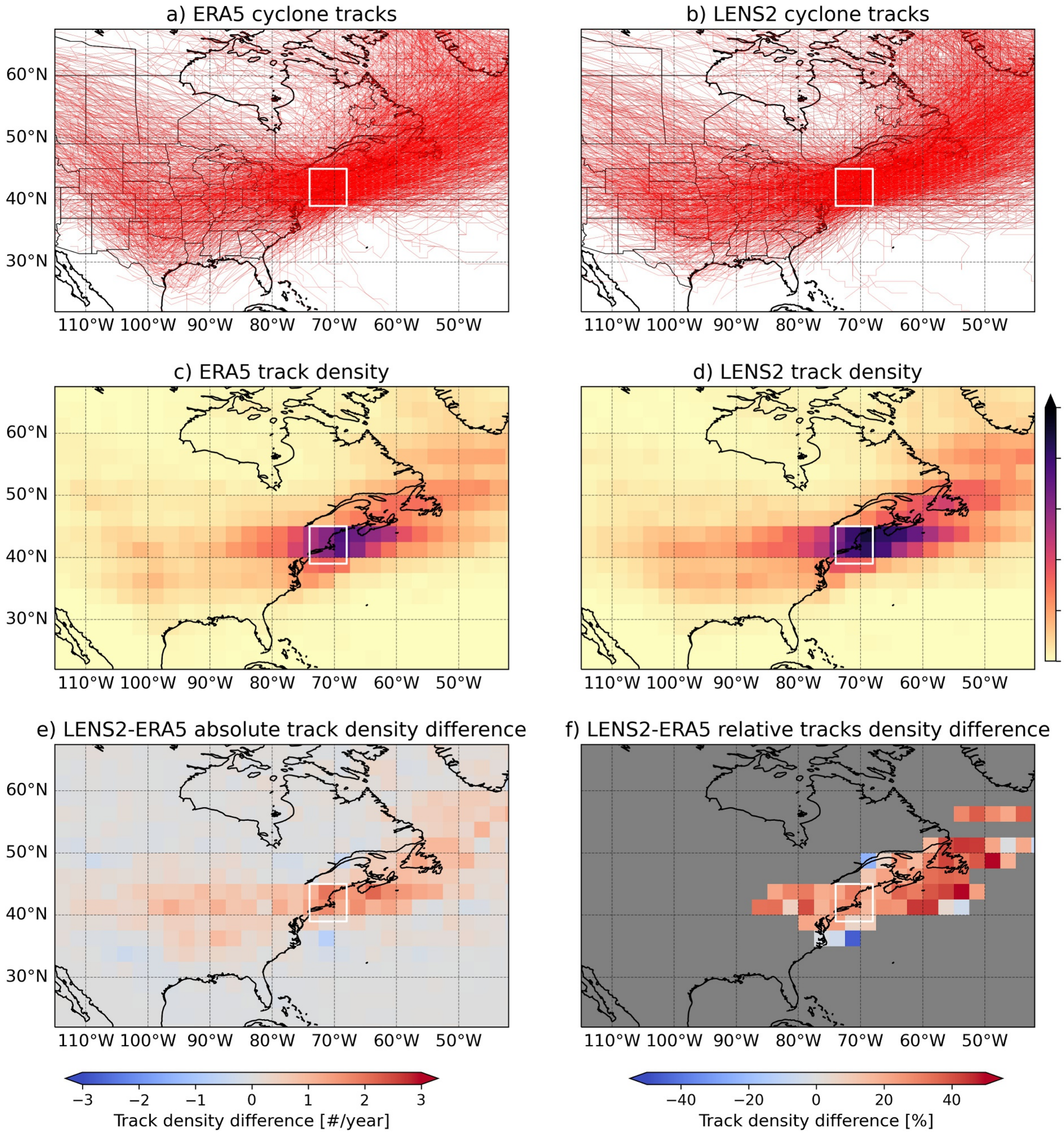

Figure 2. (a, b) The cyclone tracks for the storms passing through the region of interest (white box) along the Northeast US and (c, d) the cyclone track density for ERA5 (left), as compared to a single ensemble member (member #13) in LENS2 (right). (e, f) Absolute and relative difference in cyclone track density between LENS2 and the ERA5 ensemble member (representative of the ensemble mean). Relative differences are only shown in areas with more than 1.5 extratropical cyclones per year.

Additional simulations were then conducted to test whether to use minimum pressure or maximum wind speed as proxies for cyclone intensity when selecting cases to downscale results in stronger storms. Given our interest in identifying changes in wind hazards in the northeast US region, the maximum wind speed was used as a proxy to select the most intense ETCs. A total of 200 ETCs were simulated with MPAS for each of the following time periods: 1991–2020, 2031–2060 and 2070–2099, resulting in an ensemble of 600 downscaled ETCs. Since these simulations are initialized with LENS2 MOAR, the future simulations continue to use the SSP370 radiative forcing emissions pathway.

Following the protocol established during the mesh testing phase, each MPAS simulation was initialized 24 hr prior to the time of maximum wind speed and minimum central pressure near Boston that was identified in the

LENS data set. Meteorological fields from LENS at the initialization time were converted into WRF Preprocessing System intermediate files. These files were then processed using the MPAS init_atmosphere program to remap the data onto the 60-3 km variable-resolution mesh, generating the final initialization files. For each of the 600 selected storms, MPAS was integrated forward for three days to evaluate storm evolution.

2.5. Tracking and Evaluating ETCs in MPAS

ETCs in MPAS are tracked using the TempestExtremes TC tracker (Ullrich & Zarzycki, 2017; Ullrich et al., 2021). While ETCs in LENS2 were tracked with MOAAP, the two approaches and methods therein result in similar tracks during the phase where the cyclones are intense (deep low pressure), in line with previous findings (Neu et al., 2013; Prein et al., 2023). TempestExtremes was chosen to track the downscaled runs from MPAS as it can be used to track features on the irregular native MPAS grid, whereas MOAAP cannot. TempestExtremes is a unified, open-source framework available on github designed for feature tracking that can be used on a wide array of structured or unstructured grids, such as the variable resolution MPAS grid used in this study. The code is an automated pointwise feature tracking, an algorithmic technique for objective identification and tracking of meteorological features such as ETC, tropical cyclones, and tropical easterly waves. The tracking process focuses on (a) locating candidate points of local extremes such as minimum pressure and wind speed; (b) eliminating candidate points that do not satisfy a prescribed set of thresholds such as a prescribed regional area; (c) connecting candidate points in time; and (d) eliminating tracks based on chosen a duration criterion.

As noted by Ullrich and Zarzycki (2017), it is important to highlight that there currently is no single tracking algorithm available that provides both perfect detection and zero false alarms. The tracking criteria in this method were developed to optimize cyclone detection and minimize the false alarm rate. These ETC feature tracking criteria are employed here and include: (a) Located candidate points in the our area of interest (at least one point north of 27°N, at least one point west of −60°W and all points east of −96°W) by tracking local sea level pressure minima; (b) Eliminated candidate points that fail both a closed contour criteria (an increase of at least 2 hPa within 6° of the candidate); (c) Remaining candidate points are connected in time; (d) Tracks shorter than 18 hr are eliminated; and (e) Only tracks within the ETC season (September to April) were considered.

Extreme ETC events were evaluated to assess changes in intensity and storm structure. To investigate structural changes in the most intense cyclones, we selected a subset of the 10 most intense ETCs in each time period and created composites of the wind speeds at the surface (10 m), 850, 500, and 250 hPa levels, following methods similar to those in Priestley and Catto (2022). Cyclones are rotated to standardize their direction of movement so that the cyclones propagate eastward. Storm composites are created at the time of the maximum wind speed and cover an area of 40 × 40° from the track point at the time of maximum wind intensity.

3. Results and Discussion

3.1. Evaluating Cyclone Frequency and Characteristics Under Recent Climate Conditions

First, we evaluate the LENS2 skill at simulating ETCs under recent climate conditions for the period 1940 and 2019. Generally, cyclone tracks are well captured in LENS2 for this period. Figures 2a and 2b show the ERA5 and LENS2 cyclone tracks for all the storms that pass through the region of interest, respectively. Results reveal a similar pattern of storm tracks and track densities in both data sets. Considering all cyclones, on average the mean annual cyclone frequency in LENS2 is higher than in ERA5 by four cyclones, with a mean of 22 and 26 cyclones in ERA5 and LENS2, respectively (Figure 3e). Comparing the storm track density (Figures 2c–2f) within the region of interest, on average LENS2 overestimated the number of yearly cyclones by 23.6%.

The average monthly cyclone frequency also highlights similar patterns between cyclones in both data sets, with differences in cyclone frequency being ≤1 and with maxima and minima during winter and summer, respectively (Figure 3f). However, cyclones in LENS2 are offset by one to 2 months in terms of the time of maximum and minimum (Table 1). The minimum in ERA5 occurs in July, while in LENS2 it occurs in August. Similarly, the maximum in ERA5 is observed in January, while for LENS2 it is in March.

We additionally compared the characteristics of the storms, which show that cyclone minimum pressure, translation speed and cyclone size are well-captured in LENS2 (Figures 3a–3c). A single ensemble member is

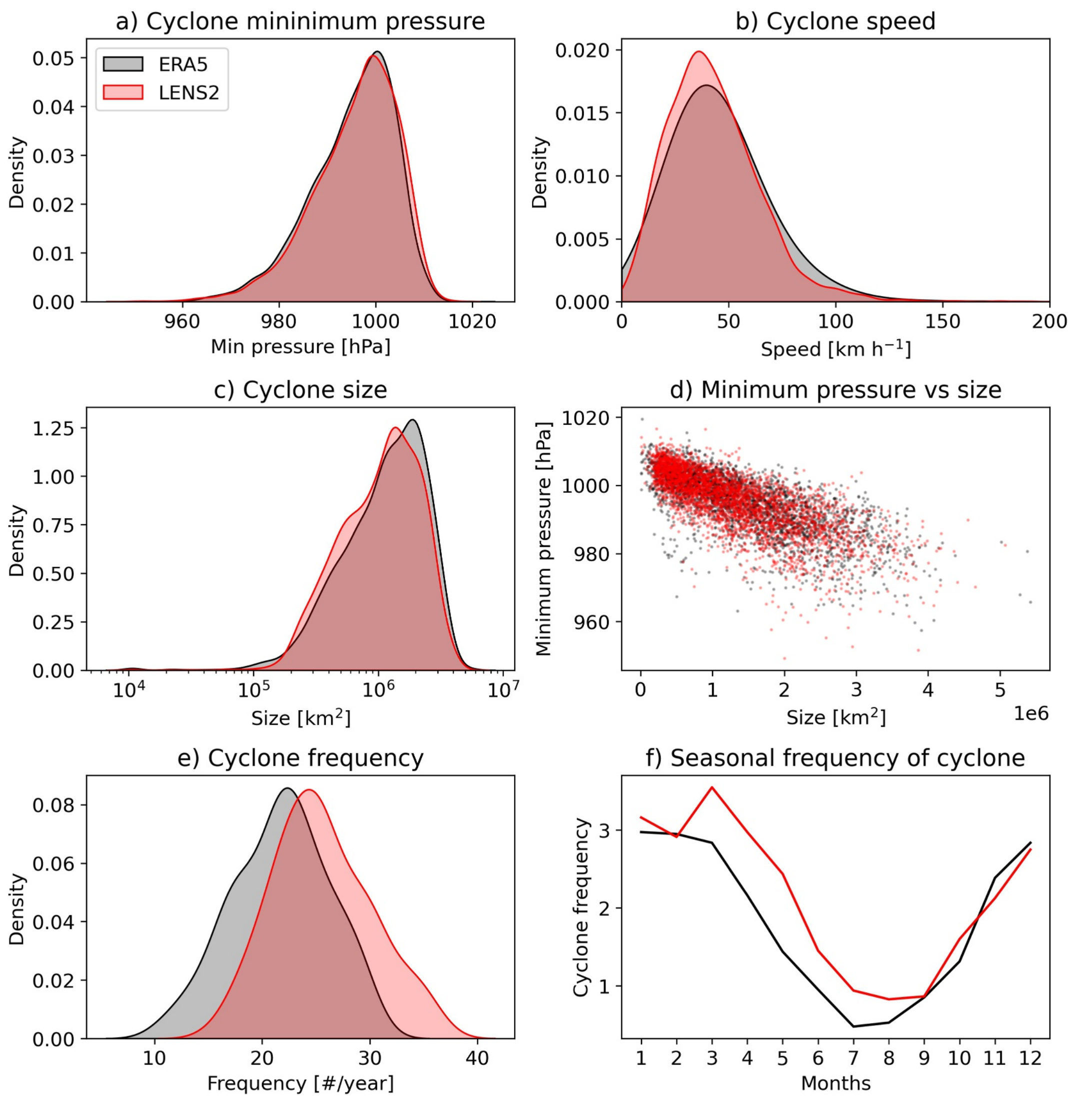

Figure 3. Comparison of storm characteristics between ERA5 (black) and LENS2 member 13 (red). PDFs of cyclone (a) minimum pressure, (b) translational speed and (c) size are shown; (d) Scatter plot of cyclone minimum pressure and storm size; (e) Yearly and (f) monthly frequency of observed cyclones.

used for comparison purposes since the results for other members are similar. Particularly, the cyclone minimum pressure is very well captured in LENS2 with the median difference to ERA5 being less than 1 hPa. Also ETC movement speed is similar in both data sets with median differences being smaller than 4% and non-significant.

Table 1
Mean Storm Characteristics in ERA5 and LENS2

	ERA5	LENS2
Minimum pressure (hPa)	995.1	995.8
Translation speed (km/hr)	46.6	42.9
Size (x 1e^6 km^2)	1.4	1.2
Monthly frequency (min/max)	July/Jan	Aug/Mar
Annual frequency	21.7	25.6

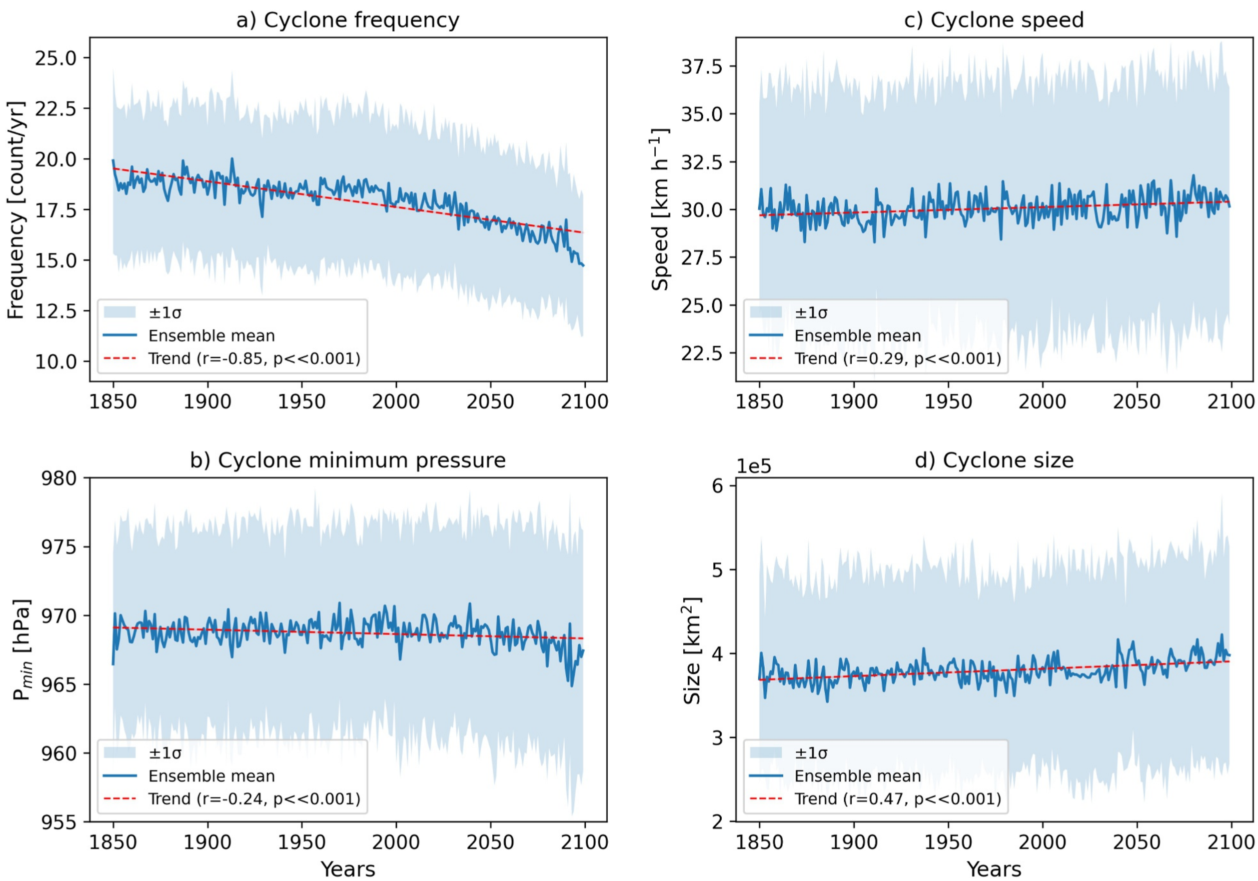

Figure 4. Projected changes in LENS2 for cyclone (a) frequency and (b) intensity, (c) speed and (d) size through the end of the century for cyclones passing through the Northeastern U.S. In each subplot, the thin blue lines represent individual 100 ensemble members and the thick lines indicate the ensemble mean. The Pearson correlation coefficient (r) of the mean cyclone characteristics with time is indicated for each parameter.

3.2. Projected Changes of Extreme ETCs in LENS2

Over the period from 1850 to 2100, the average annual cyclone frequency is roughly 18 per year (Figure 4a). Future cyclone projections under an SSP3-7.0 emission scenario, indicate a decrease in the annual number of ETCs, with an average of 16 cyclones for the end of the century (2070–2099), consistent with previous findings (Priestley & Catto, 2022; Sinclair et al., 2020). This decreasing trend in average cyclone frequency over time, also indicated by a significantly strong negative correlation coefficient, is also characterized by a decrease in variability among ensemble members. Monthly frequency projections for the 30 most intense cyclones in each LENS2 member (Figure 5b) show a seasonal shift in extreme ETCs. By end of century, storm frequency increases by an average of 0.46 storms over the winter months (December–February) and decreases by 0.41 storms during spring (March–May), relative to the 1990–2020 baseline period. A similar trend is observed for mid-century as compared to the current period but with a narrower window with increases concentrated over December-January and decreases during April-May. The cyclone translation speed and size (Figures 4c and 4d) trends show a weak and moderate positive correlation, respectively. The projected increase in cyclone size is more noticeable and with lower variability among ensemble members than projected changes in cyclone speed.

Projected changes in cyclone intensity show a less robust trend than cyclone frequency, with a small decrease in minimum pressure (increased intensity) by the end of the century but increasing variability among the different ensemble members for the end of century (2050–2100) period (Figure 4b). Compared to the 1850–2050 time period, the standard deviation increases by (0.72σ).This is indicated by a weak but statistically significant correlation.

In Figure 5a, results show that the minimum cyclone pressure of rare events is expected to decrease in the future. What is considered a 1 in 100-year event for past and recent climate conditions, with a return value of cyclone

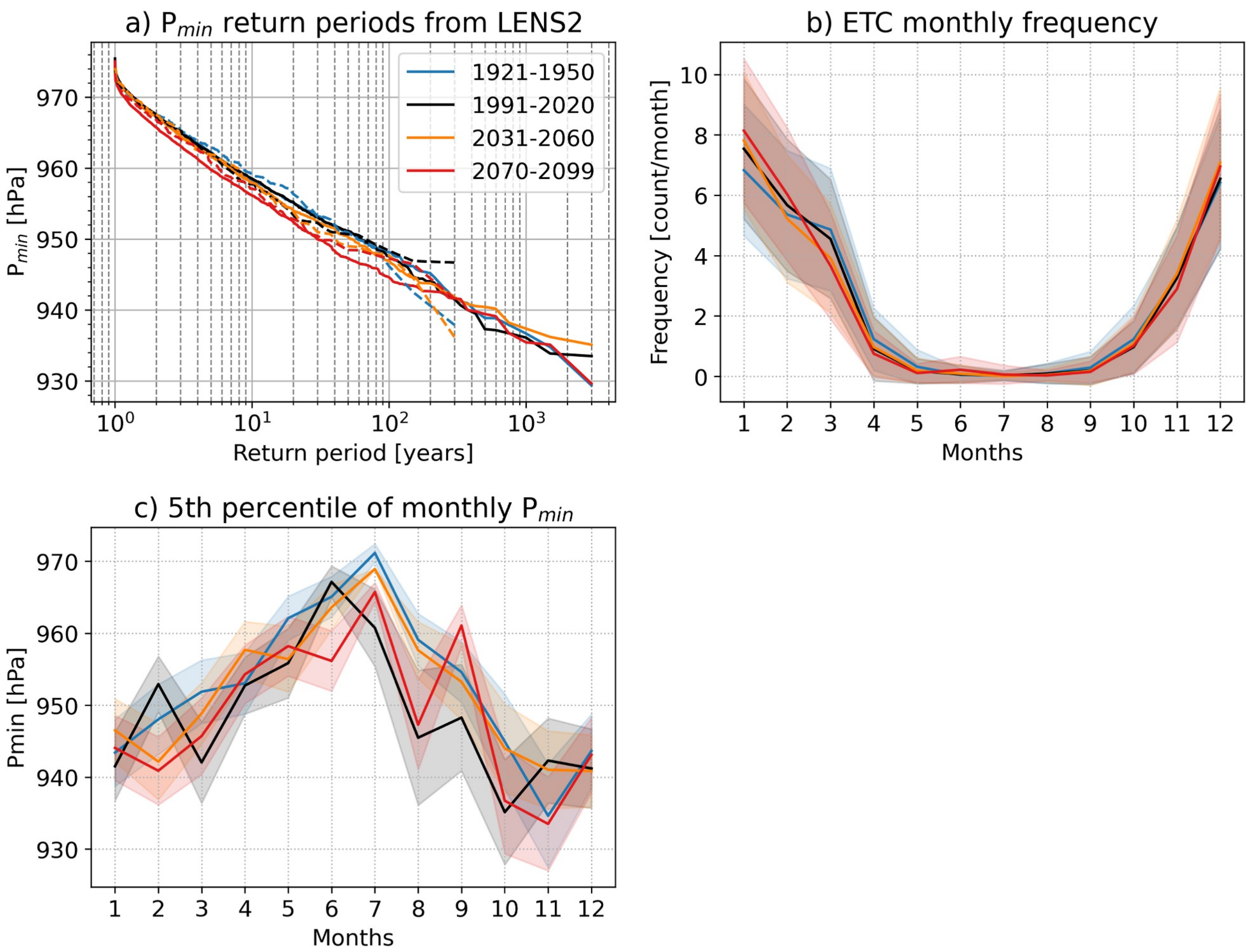

Figure 5. (a) Return values of cyclone minimum pressure within the region of interest. The solid lines account for values from the 100-member LENS ensemble and the dashed lines represent the 10-member MOAR simulations. (b) Monthly frequency of extratropical cyclones per time period and (c) 5th percentile of monthly minimum pressure. These figures consider the 30 most intense cyclones, as given by the minimum pressure, for each time period and each LENS2 member. Shading in panels (b–c) indicate standard deviation.

minimum pressure of 948 mb, is projected as a 1 in 40-year event under future climate projections. The projected return value of cyclone minimum pressure for a one in 100-year event for the 2070–2099 period is roughly 944 mb. The signal is similar but noisier for the MOAR simulations due to their smaller ensemble size. ETC-associated pressures are lowest/more intense between the months of October and December (Figure 5c).

Projections of ETC storm track density for the mid- and end-of-century time periods, as compared with recent climate conditions, provide further insights into the projected frequency and intensity changes of ETCs, as well as changes in storm tracks. With respect to the region of interest, the frequency of all ETCs impacting this area is shown to gradually decrease with time (Figures 6c, 6e, and 6g). Significant changes are expected toward the end of the century within the region of interest and extending zonally from there. However, the frequency of the most intense storms is shown to significantly increase within the region of interest. Changes in the annual maximum frequency show another key feature, more prominent in the end-of-century projections, of a decrease in the zonal pathway of storms (e.g., from the Midwest to the Northeast) and an increase in storms that track through the Southeast U.S. coming up the Atlantic seaboard. Projected changes point to increasing exposure to ETC produced winds and precipitation in the Northeast US region.

3.3. Downscaled Extreme ETC Events

The top 100 most intense ETC events identified in LENS2 MOAR in the 30-year current, 30-year mid-century and end-of-century periods were selected according to the maximum wind speed over the Boston region, resulting

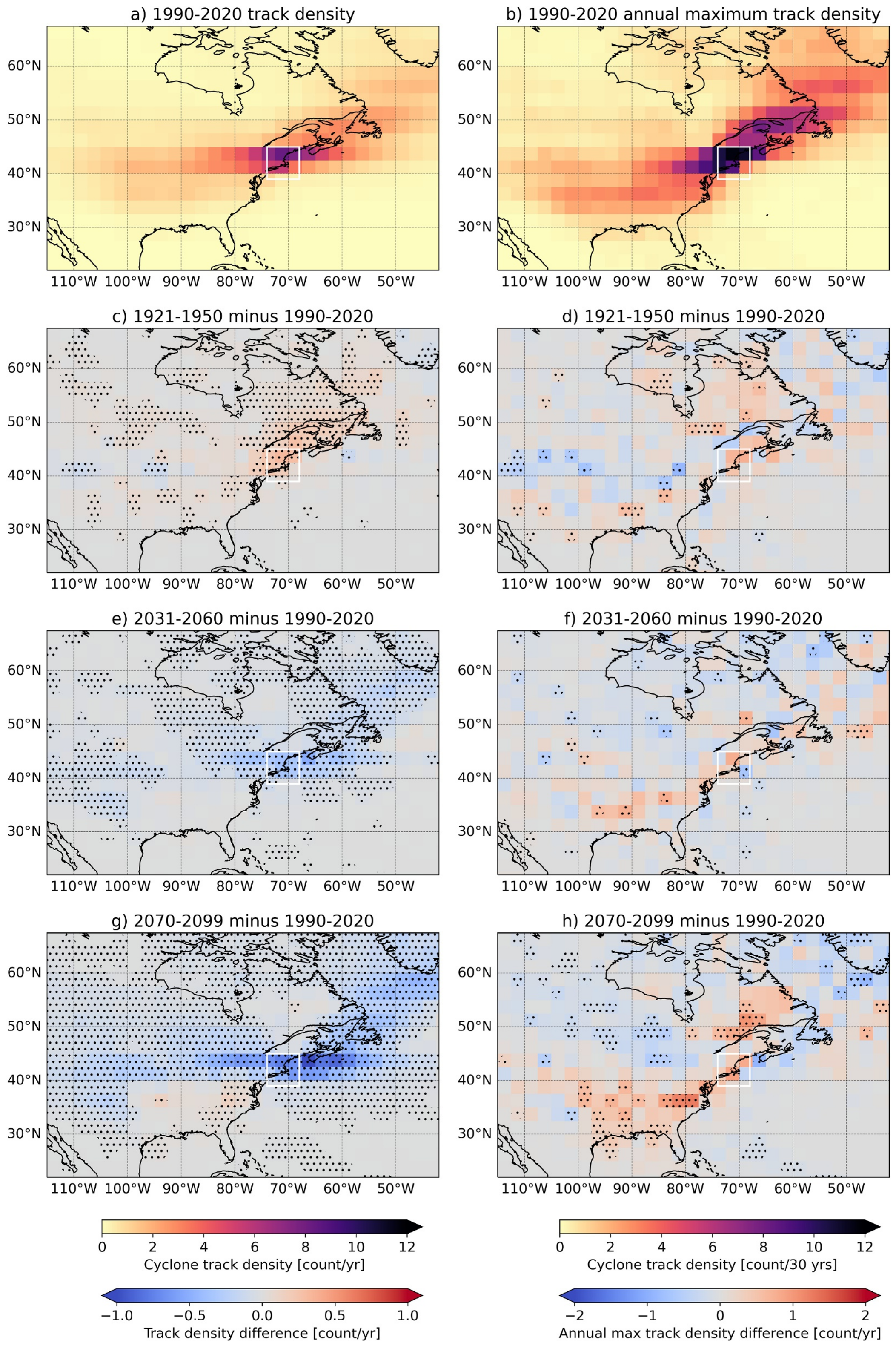

Figure 6. (a) Mean and (b) annual maximum storm track density of cyclones passing through the region of interest (white square) for the 1990–2020 period and differences in mean track density between (c, d) past climate, (e, f) mid-century projections and (g, h) end-of-century projections from current climate. Panels on the left represent all cyclones passing through the region of interest and panels on the right represent the top 30 most intense cyclones per period. Hashing indicates statistically significant changes at the 0.05 significance level.

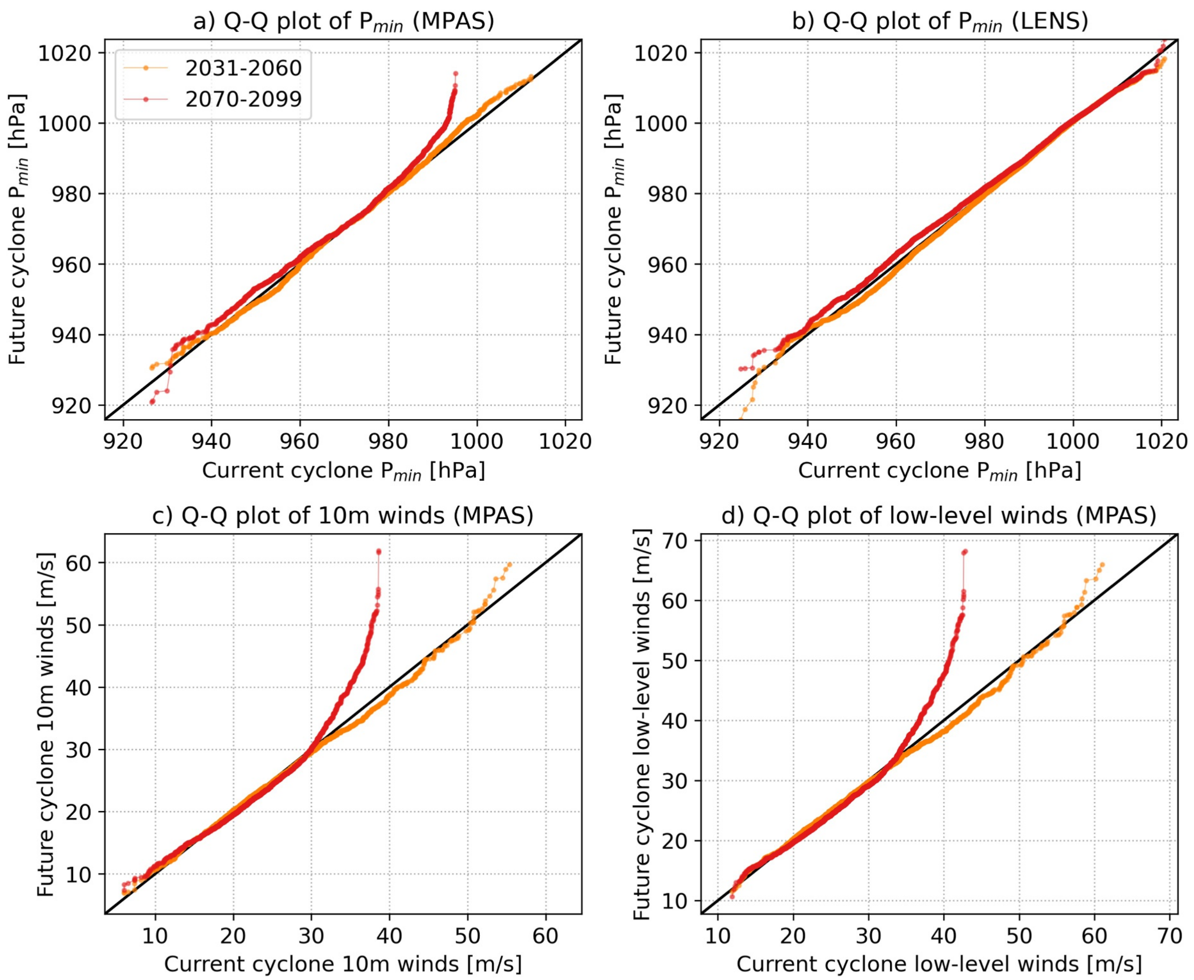

Figure 7. Quantile-quantile (Q-Q) plots of future versus present-day extreme cyclones downscaled with model for prediction across scales showing cyclone (a) minimum pressure, (b) 10-m winds and (c) low-level winds. (b) Equivalent to (a) for cyclones in LENS2.

in an MPAS-downscaled ensemble of 300 storms. Examining these intense cyclones, the environment they interact and develop in, and how these are expected to change in the future provides a better understanding of the potential wind impact in the region of interest due the enhanced simulation of dynamical processes, coastlines, and land surfaces at 3 km grid spacing in MPAS.

While the present analysis of the MPAS simulations cannot discern changes in frequency, we can comment on projected changes in storm intensity. Projections of ETC intensity in the literature span the full range of possibilities, in part due to competing environmental factors influencing ETC intensity such as changes in low-level baroclinicity, shifts in the position of the polar or subtropical jet stream and changes in moisture availability (Chen et al., 2025; Colle et al., 2015; Lynne & Dai, 2025).

Figures 7a and 7b provides insight into minimum pressure trends depicted by MPAS and LENS2 by comparing the distribution of extreme cyclone minimum pressure and maximum wind at different levels for future periods with that of the 1990–2019 period. Results indicate that the bulk of the distribution, between 940 and 990 mb, isn't expected to change much. Notably, results show that the most intense cyclones (below ~940 mb) may become even stronger by the end of the century. This signal is not evident when evaluating the LENS2 results as the curves for both periods closely follow the 1:1 line across nearly the entire range. There is only a slight deviation at the extreme low end of the pressure range. The contrast between the results shown in Figures 7a and 7b underscore the value of using a model like MPAS for ETC intensity proejctions. Results in Figures 7c and 7d also indicate intensification of the 10 m and low level wind speeds. These trends are more evident for the end-of-century period. Examining the 10-m maximum wind speed return period in Boston, MA (Figure 8), results indicate

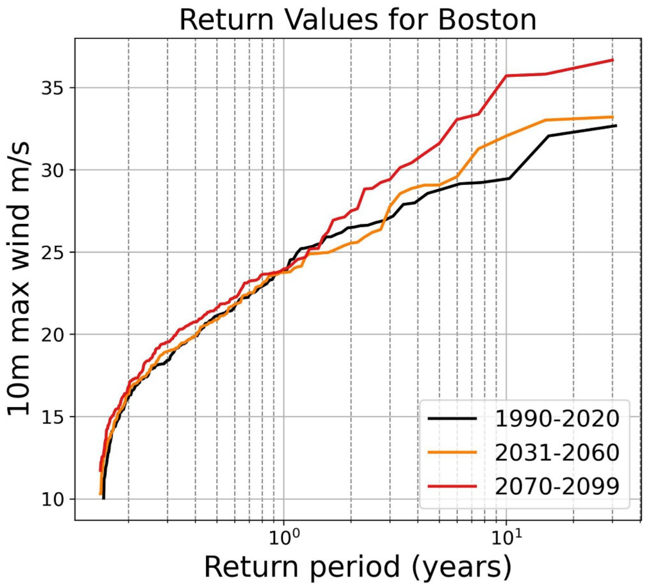

Figure 8. Return values of the 10 m maximum wind speed for Boston, MA. The data presented includes values for the nearest 25 grid cells to the point of interest.

higher wind speeds for the same return periods in the future projections, mainly for the end-of-century period, highlighting a heightened risk of extreme wind events. Notably, while there are fewer changes in the short-term, the low-frequency events show the largest increases in wind speeds.

Figure 9 shows the MPAS-derived 850 mb temperature averaged for the 100 most intense ETCs at the time of maximum wind. While not shown, the depiction of temperature in MPAS for each time period is consistent with that of LENS2. Results indicate that the thermodynamic environment of the most intense ETCs is changing substantially under future climate conditions, generally warming along the Atlantic seaboard. Using the ±5°C isotherm as reference, results show a poleward displacement of the cold air mass. We took three ~1400 km transects along the temperature gradient, oriented northwest-southeast and cutting across the land-ocean boundary, to evaluate the changes in temperature gradient. Across all transects, the 850 mb temperature remained relatively constant across the three time periods with slopes differing no more than 0.05°C/100 km. These results suggest that while the environment warms overall, the baroclinic zone shifts poleward and the baroclinicity is preserved in the future. The storm track shift observed in Figure 6 can be due in part to the poleward migration of this baroclinic zone.

We additionally subset the top 10 most intense cyclones from the MPAS data set for each time period and examined changes in their 3-dimensional spatial and thermodynamic structure. Figure 10 depicts composites of wind speeds at the surface (Figure 10a), 850 hPa (Figure 10d), 500 hPa (Figure 10g) and 250 hPa (Figure 10j) levels for the present time period, and projected structural changes of the cyclones for mid (Figure 10 middle column) and end-of-century (Figure 10 right column). Note that prior to compositing, the cyclones are rotated to standardize their direction of movement, and results are herein described in relation to the cyclone motion (eastward/right of the

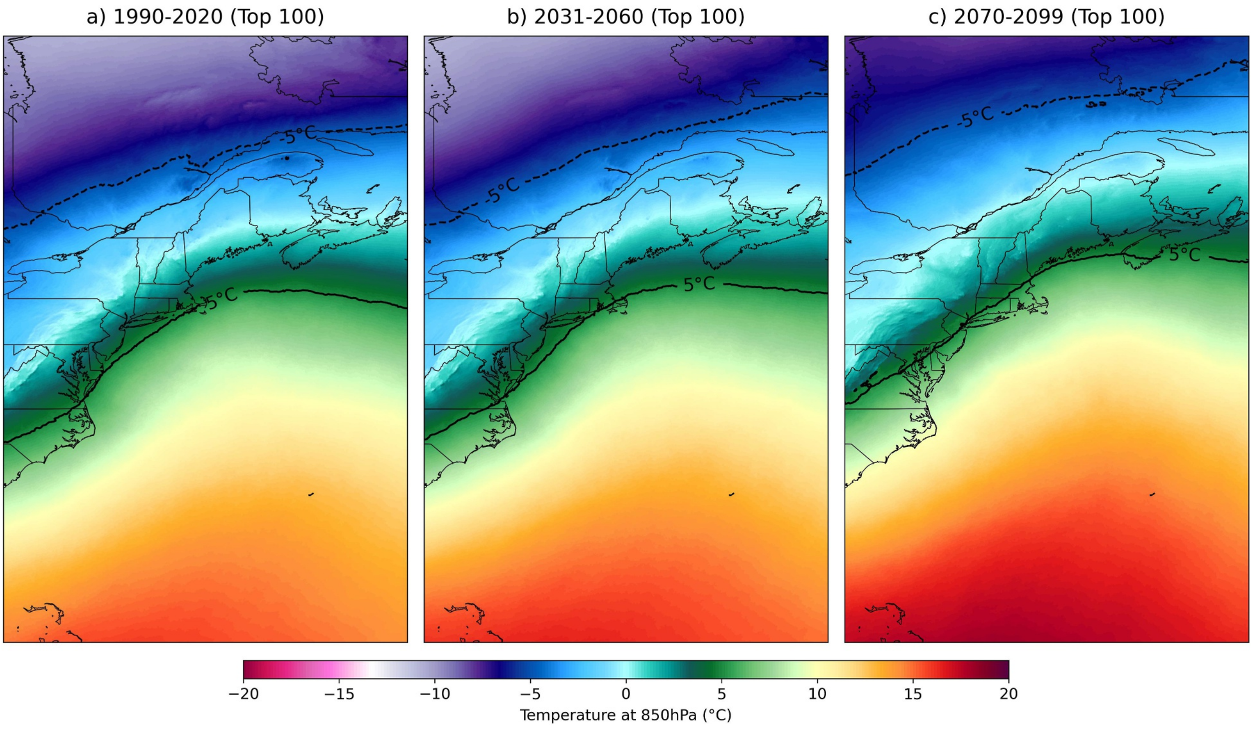

Figure 9. MPAS-derived 850 mb temperature averaged for the 100 most intense extratropical cyclone events for the (a) 1990–2020, (b) 2031–2060 and (c) 2070–2099 periods. Panels (d and e) show the relative shift from the 1990–2020 reference period. The −5°C (dashed black line) and 5°C (black line) isotherms are plotted for reference.

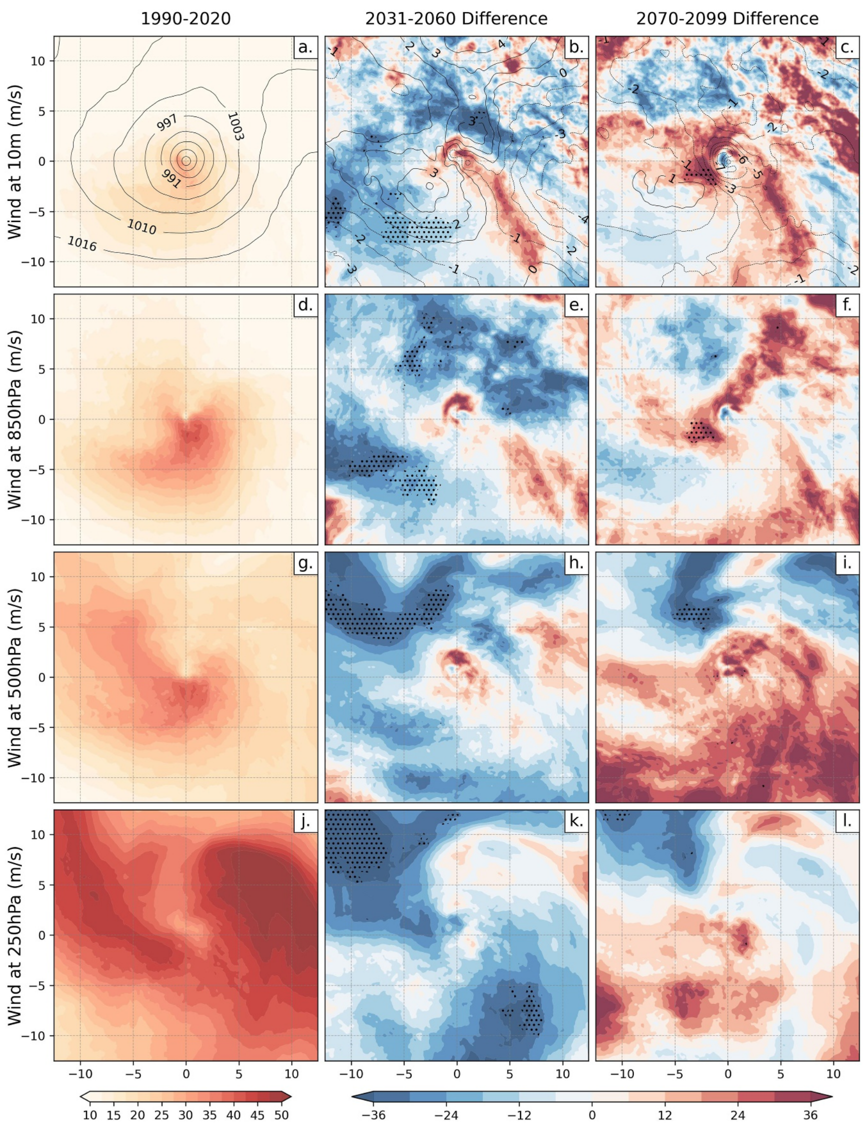

Figure 10. MPAS-derived wind speed composites at the time of maximum wind speed for the current time period (left panels) and percent differences from the current time period at (a–c) lower levels (10 m), (d–f) 850 hPa, (g–i) 500hP and (j–l) 250 hPa levels of the 10 most intense Extratropical Cyclones based on maximum wind speed. Black contours on top panels represent mean sea level pressure (left) and absolute differences from the current time period (middle and right panels). Hashing indicates statistically significant changes at the 0.05 significance level.

plots). The same storms were also subset from the LENS2 data set for comparison purposes with MPAS (Figure 11). Broadly, the LENS2 derived storms are weaker than projected with MPAS. Results for the top 20 cyclones for each data set are shown in Figures S4 and S5 in Supporting Information S1.

Generally, changes from the present to mid-century to late century are not monotonic. At the surface, MPAS results show strengthening of winds immediately around the storm center for both mid and end-of-century projections (Figures 10b and 10c). There is a notable increase in winds to the rear of the storm center, more prominent, and significant in the lower right quadrant, in end-of-century, which is not captured in LENS2 (Figure 11c). The dipole in the change field at the composite center also suggests a tightening of gradients within the storm. MPAS results also indicate strengthening winds to the upper right of the storm from the storm center, similar in findings from Priestley and Catto (2022) for winter time storms. This effect is then combined with a broadening of the areas with high winds. These patterns are not captured with LENS2, particularly the increasing winds in the upper left quadrant.

10.1029/2026JD046823

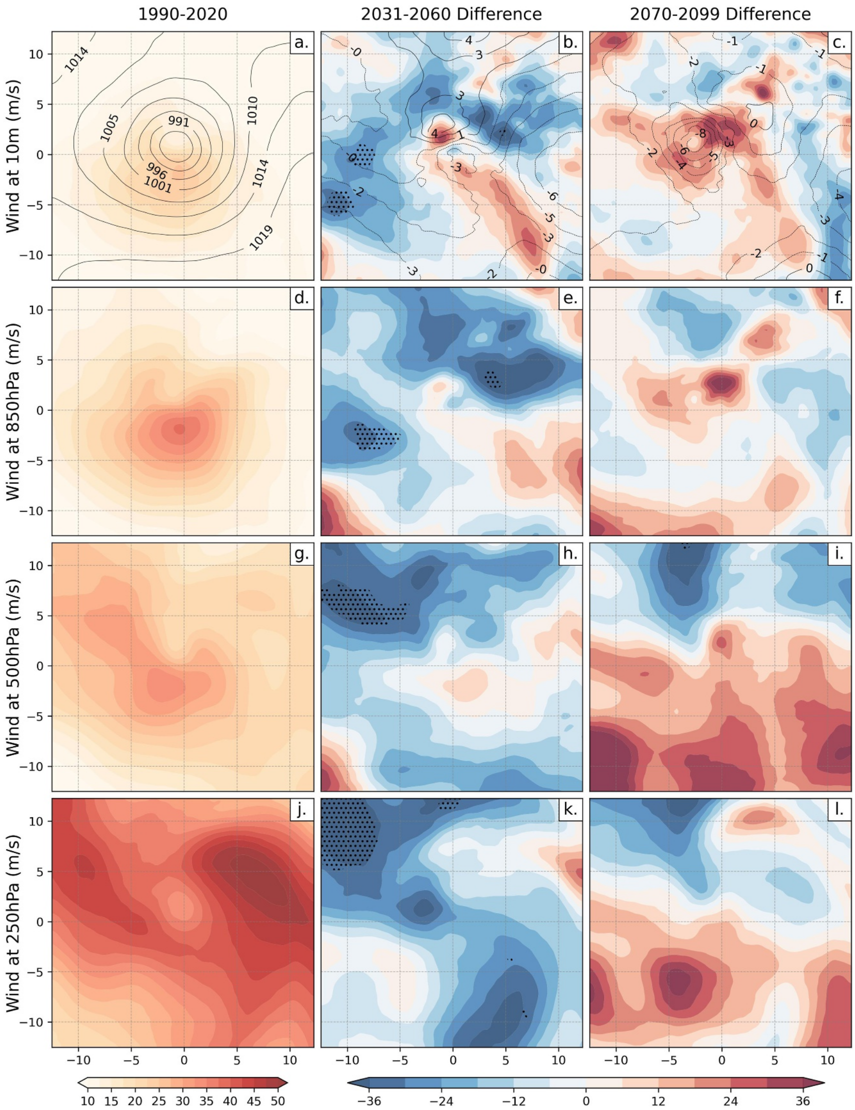

Figure 11. Same as Figure 10 but showing LENS2-derived data for the same storms.

At the 850 mb level, MPAS simulations show signs of increasing winds mainly located around the left quadrants of the cyclone cores for mid-century (Figure 9e), not captured in LENS2. Results also show significant decrease in winds in the lower quadrants in the far-field for mid-century, and indicate intensification and broadening of the wind field in the upper quadrants beyond the storm center toward the end-of-century.

Differences in wind composites for the mid level at 500 hPa, show more pronounced differences between mid and end-of-century changes, evident in both LENS2 and MPAS. For the mid century, MPAS-derived differences (Figure 10h) show projected strengthening surrounding the storm center, that is more pronounced in the left quadrants– a feature not captured in LENS2 (Figure 11h). Results also show significant weakening winds in the lower left quadrant away from the storm center, evident in both data sets. For the late century, projections largely show increasing winds surrounding the storm center in all quadrants, and in the far field in the right quadrants. Weakening winds are evident for the outer lower left quadrant (Figure 10i).

At the 250 hPa level, we see an interaction of the jet stream and the upper levels of the storm. The future change maps suggest a rotation of the orientation of the low-level composite storm relative to the upper level trough. This is shown in the winds that are projected to decrease to the upper right and lower left storm quadrants during the 2031–2060 period (Figure 10k). This overall pattern is captured in LENS2 simulations as well. However, for the

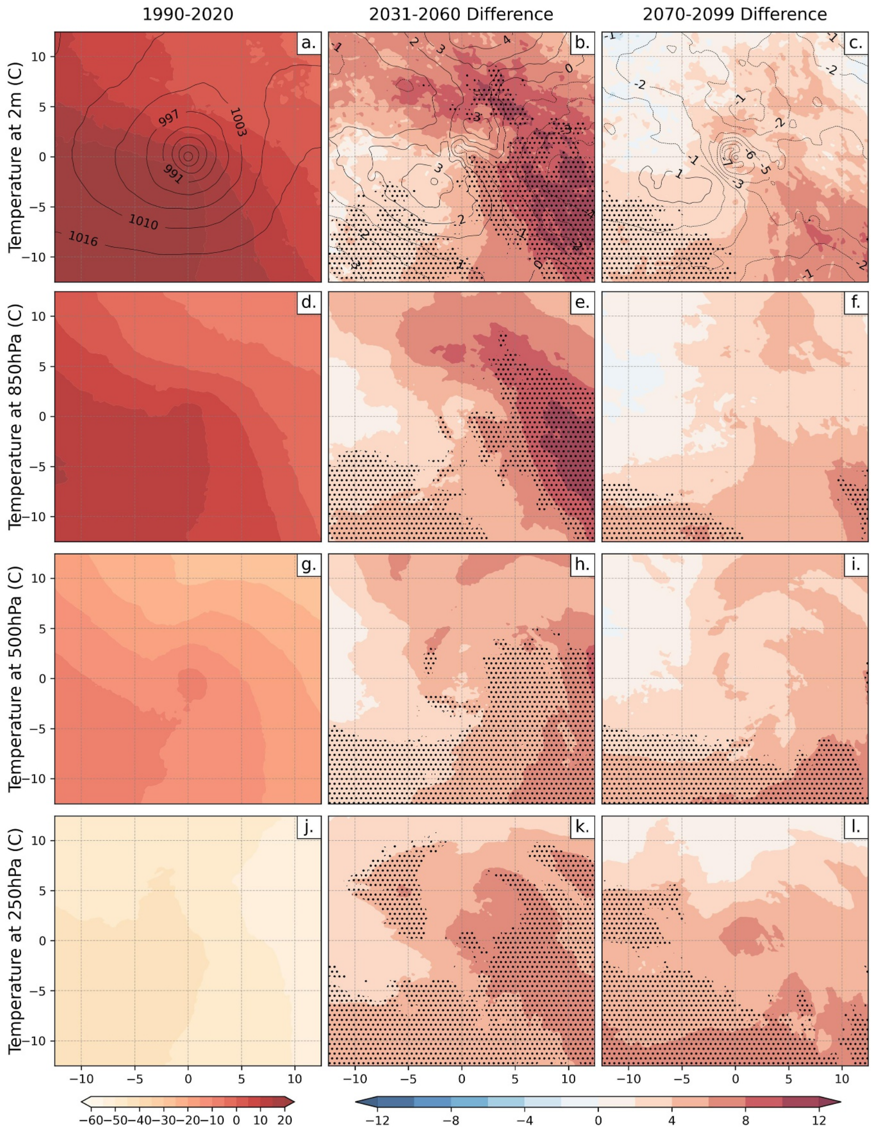

Figure 12. MPAS-derived temperature composites at the time of maximum wind speed for the current time period (left panels) and absolute differences from the current time period at (a–c) lower levels (10 m), (d–f) 850 hPa, (g–i) 500hP and (j–l) 250 hPa levels of the 10 most intense extratropical cyclones based on maximum wind speed. Black contours on top panels are mean sea level pressure (left panel) and absolute differences from the current time period in middle and right panels. Hashing indicates statistically significant changes at the 0.05 significance level.

end of century projections (Figure 10l), while the weakening in the lower left quadrant remains, results indicate an increase in winds along the right quadrants, also consistent with Priestley and Catto (2022). LENS2 simulations generally capture the increasing pattern in the right quadrants but not near the cyclone center.

Figure 12 depicts composites of temperature at the surface (2-m height; Figure 12a), 850 hPa (Figure 12d), 500 hPa (Figure 12g) and 250 hPa (Figure 12j) levels for the present time period, and projected changes of the cyclones for mid (Figure 12 middle column) and end-of-century (Figure 12 right column). Results show that higher temperature air is advected into the cyclone in the warm sector, while the cold sector does not warm as much. This indicates that there is more moist warm air advection and that the temperature gradients in the cyclone are increasing with warming, ultimately resulting in stronger cyclones. This agrees with our results that more cyclones are tracking from the southeast in the future climate. The MPAS and LENS2 results seem to agree overall.

10.1029/2026JD046823

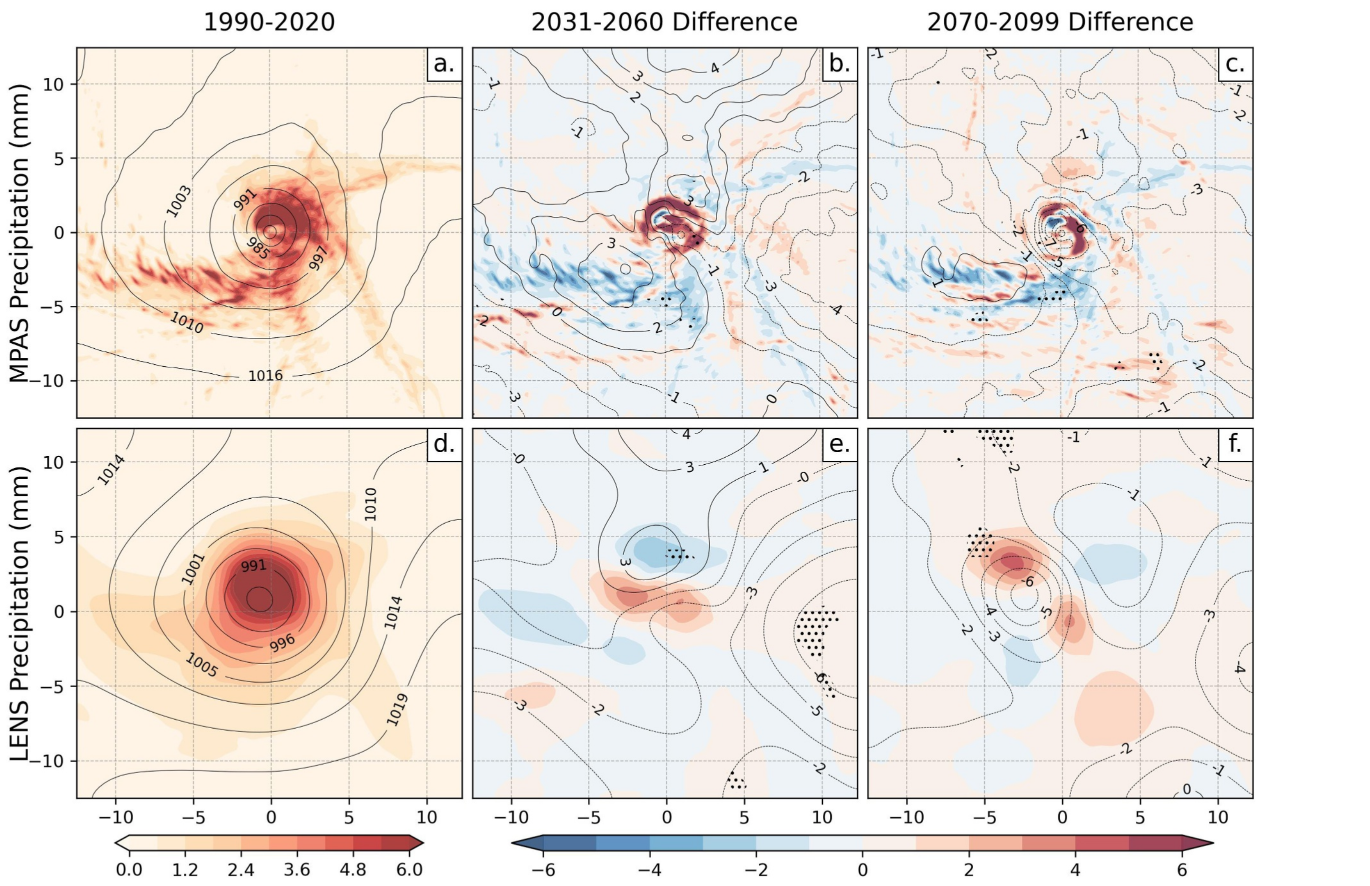

Figure 13. MPAS-derived precipitation composites at the time of maximum wind speed for the current time period (left panels) and absolute differences from the current time period of the 10 most intense extratropical cyclones based on maximum wind speed. Black contours are mean sea level pressure (left panels) and absolute differences from the current time period in middle and right panels.

Figure 13 shows the precipitation associated with the top 10 most intense ETCs. The MPAS simulations (Figure 13a) provide a more realistic representation of the ETC precipitation structure including intense precipitation northeast of the storm center and depicting the frontal rainbands associated with ETCs. The precipitation structure depicted in LENS (Figure 13d) is less detailed and almost symmetrical, highlighting the value added of the downscaling process. Examining the MPAS projections, these point to differences in where precipitation changes concentrate, suggesting increasing precipitation (>6 mm) along the storm center and decreasing precipitation in the frontal bands. Generally, this pattern is consistent with a stronger, tighter storm structure driven by enhanced latent heat release (Chen et al., 2025). Additionally, consistent with the environmental temperature findings discussed, these changes are not monotonic with time.

4. Conclusions

The study examined changes in mid- and end-of-century ETC characteristics leveraging the CESM2 Large ensemble data set (LENS2) and downscaled simulations with the MPAS model. The main findings of our work are as follows:

- CESM LENS2 proved skillful in simulating historical ETC frequencies and characteristics as compared to ERA5. Results indicate that while the frequency of ETCs is projected to decrease under future climate conditions, the minimum pressure and maximum low-level winds of extreme ETCs are projected to intensify. This trend is further supported by the downscaled simulations, showing that the maximum 10 m wind speeds and maximum low-level winds of the most extreme cyclones increase 28% from the current time period to the end of the century.

- A shift in track is projected for future extreme ETCs characterized by decrease in the zonal pathway of storms (e.g., from the Midwest to the Northeast) and an increase in trajectories through the Southeast U.S. moving north along the Atlantic seaboard.
- The current climate 100 years storm is projected to double in frequency and occur every 40 years at the end of the century.
- Composites of the 10 most intense cyclones in MPAS were used to assess changes in the 3D wind field structure across time periods. Overall, MPAS projects non monotonic yet increasingly intensified and broadened wind field changes from the present to mid-century to late century. LENS2 is able to capture some of the large-scale structural patterns, but generally has lower wind intensity and associated structural changes than found in LENS2.
- Composites of the 10 most intense cyclones in MPAS were also used to assess changes in the temperature structure across time periods. Results show that warming leads to increased advection of warm, moist air and steeper temperature gradients within cyclones, driving an intensification of cyclones.

Despite the significance of these findings, it is important to note an inherent limitation of the study. The study mainly focuses on cyclones that move through a target region in the vicinity of Boston, MA and the result should be interpreted in that context. While this initial study focuses on wind hazards from ETCS, there are a number of additional applications for the data generated including, evaluating the pressure-intensity relationship for ETCs, identifying and evaluating ET transitions, simulating storm surge impacts and further evaluating precipitation impacts from ETCs and their projected future changes.

Conflict of Interest

The authors declare no conflicts of interest relevant to this study.

Availability Statement

The MPAS model is open source and can be downloaded from MPAS (2025). The CESM LENS2 data set is available from the NSF NCAR Geoscience Data Exchange (Danabasoglu, Deser, et al., 2020). The MPAS simulations evaluated in this study can be accessed at Jaye (2025) through Globus. Access of the simulations through Globus requires login using ORCID or an institutional email.

Acknowledgments
This material is based upon work supported by Plymouth Rock Home Assurance Corporation and the NSF National Center for Atmospheric Research, which is a major facility sponsored by the U.S. National Science Foundation under Cooperative Agreement No. 1852977. The views and conclusions expressed herein are those of the authors and do not necessarily reflect the views of the funding agencies. The authors acknowledge James Done for constructive feedback on an earlier draft of this manuscript.

References

Blender, R., Fraedrich, K., & Lunkeit, F. (1997). Identification of cyclone-track regimes in the North Atlantic. *Quarterly Journal of the Royal Meteorological Society*, *123*(539), 727–741. https://doi.org/10.1002/qj.49712353910

Catto, J. L., Ackerley, D., Booth, J. F., Champion, A. J., Colle, B. A., Pfahl, S., et al. (2019). The future of midlatitude cyclones. *Current Climate Change Reports*, *5*(4), 407–420. https://doi.org/10.1007/s40641-019-00149-4

Chen, K., Li, X., Weaver, M. M., Christiansen, S. A., Horton, A. L., & Mann, M. E. (2025). The intensification of the strongest nor'easters. *Proceedings of the National Academy of Sciences*, *122*(29), e2510029122. https://doi.org/10.1073/pnas.2510029122

Colle, B. A., Booth, J. F., & Chang, E. K. (2015). A review of historical and future changes of extratropical cyclones and associated impacts along the US East Coast. *Current Climate Change Reports*, *1*(3), 125–143. https://doi.org/10.1007/s40641-015-0013-7

Danabasoglu, G., Deser, C., Rodgers, K., & Timmermann, A. (2020). CESM2 large ensemble [Dataset]. *NSF National Center for Atmospheric Research*. https://doi.org/10.26024/kgmp-c556

Danabasoglu, G., Lamarque, J. F., Bacmeister, J., Bailey, D. A., DuVivier, A. K., Edwards, J., et al. (2020). The community earth system model version 2 (CESM2). *Journal of Advances in Modeling Earth Systems*, *12*(2), e2019MS001916. https://doi.org/10.1029/2019ms001916

Eyring, V., Bony, S., Meehl, G. A., Senior, C. A., Stevens, B., Stouffer, R. J., & Taylor, K. E. (2016). Overview of the coupled model intercomparison project phase 6 (CMIP6) experimental design and organization. *Geoscientific Model Development*, *9*(5), 1937–1958. https://doi.org/10.5194/gmd-9-1937-2016

Grell, G. A., & Freitas, S. R. (2014). A scale and aerosol aware stochastic convective parameterization for weather and air quality modeling. *Atmospheric Chemistry and Physics*, *14*(10), 5233–5250. https://doi.org/10.5194/acp-14-5233-2014

He, C., Valayamkunnath, P., Barlage, M., Chen, F., Gochis, D., Cabell, R., & Ek, M. (2023). *The community Noah-MP land surface modeling system technical description version 5.0*. NCAR Technical Note NCAR/TN-575+ STR. https://doi.org/10.5065/ew8g-yr95

Hersbach, H., Bell, B., Berrisford, P., Hirahara, S., Horányi, A., Muñoz-Sabater, J., et al. (2020). The ERA5 global reanalysis. *The Quarterly Journal of the Royal Meteorological Society*, *146*(730), 1999–2049. https://doi.org/10.1002/qj.3803

Iacono, M. J., Delamere, J. S., Mlawer, E. J., Shephard, M. W., Clough, S. A., & Collins, W. D. (2008). Radiative forcing by long-lived greenhouse gases: Calculations with the AER radiative transfer models. *Journal of Geophysical Research*, *113*(D13). https://doi.org/10.1029/2008jd009944

Jaye, A. (2025). LENS/MPAS ETCs [Dataset]. *Globus*. Retrieved from https://app.globus.org/file-manager?origin_id=658134f0-f273-461e-b95a-ab2c119c2268&origin_path=%2F

Karwat, A., Franzke, C. L., Pinto, J. G., Lee, S. S., & Blender, R. (2024). Northern hemisphere extratropical cyclone clustering in era5 reanalysis and the cesm2 large ensemble. *Journal of Climate*, *37*(4), 1347–1365. https://doi.org/10.1175/jcli-d-23-0160.1

Konstali, K., Spengler, T., Spensberger, C., & Sorteberg, A. (2024). Linking future precipitation changes to weather features in CESM2-LE. *Journal of Geophysical Research: Atmospheres*, *129*(16), e2024JD041190. https://doi.org/10.1029/2024JD041190

Letson, F. W., Barthelmie, R. J., Hodges, K. I., & Pryor, S. C. (2021). Intense windstorms in the northeastern United States. *Natural Hazards and Earth System Sciences*, *21*(7), 2001–2020. https://doi.org/10.5194/nhess-21-2001-2021

Lynne, M. S., & Dai, A. (2025). Climatology, trends, and variability of cold-season northern hemisphere extratropical cyclone characteristics during 1950–2023 in ERA5. *Climate Dynamics*, *63*(12), 464. https://doi.org/10.1007/s00382-025-07956-6

Michaelis, A. C., Willison, J., Lackmann, G. M., & Robinson, W. A. (2017). Changes in winter north Atlantic extratropical cyclones in high-resolution regional pseudo–global warming simulations. *Journal of Climate*, *30*(17), 6905–6925. https://doi.org/10.1175/JCLI-D-16-0697.1

Michalek, A., Done, J. M., & Villarini, G. (2024). Future changes in regional tropical cyclone wind, precipitation, and flooding using event-based downscaling. *Earth's Future*, *12*(6), e2023EF004279. https://doi.org/10.1029/2023EF004279

MPAS. (2025). Model for prediction across scales (MPAS) [Software]. *GitHub*. Retrieved from https://github.com/MPAS-Dev/MPAS-Model

Nakanishi, M., & Niino, H. (2006). An improved Mellor–Yamada level-3 model: Its numerical stability and application to a regional prediction of advection fog. *Boundary-Layer Meteorology*, *119*(2), 397–407. https://doi.org/10.1007/s10546-005-9030-8

Nederhoff, K., Leijnse, T. W., Parker, K., Thomas, J., O'Neill, A., van Ormondt, M., et al. (2024). Tropical or extratropical cyclones: What drives the compound flood hazard, impact, and risk for the United States Southeast Atlantic coast? *Natural Hazards*, *120*(9), 8779–8825. https://doi.org/10.1007/s11069-024-06552-x

Neu, U., Akperov, M. G., Bellenbaum, N., Benestad, R., Blender, R., Caballero, R., et al. (2013). IMILAST: A community effort to intercompare extratropical cyclone detection and tracking algorithms. *Bulletin of the American Meteorological Society*, *94*(4), 529–547. https://doi.org/10.1175/bams-d-11-00154.1

Olson, J. B., Kenyon, J. S., Angevine, W., Brown, J. M., Pagowski, M., & Sušelj, K. (2019). A description of the MYNN-EDMF scheme and the coupling to other components in WRF–ARW.

Olson, J. B., Smirnova, T., Kenyon, J. S., Turner, D. D., Brown, J. M., Zheng, W., & Green, B. W. (2021). A description of the MYNN surface-layer scheme.

Pinto, J. G., Spangehl, T., Ulbrich, U., & Speth, P. (2005). Sensitivities of a cyclone detection and tracking algorithm: Individual tracks and climatology. *Meteorologische Zeitschrift*, *14*(6), 823–838. https://doi.org/10.1127/0941-2948/2005/0068

Prein, A. F., Mooney, P. A., & Done, J. M. (2023). The multi-scale interactions of atmospheric phenomenon in mean and extreme precipitation. *Earth's Future*, *11*, e2023EF003534. https://doi.org/10.1029/2023EF003534

Priestley, M. D., & Catto, J. L. (2022). Future changes in the extratropical storm tracks and cyclone intensity, wind speed, and structure. *Weather and Climate Dynamics Discussions*, *2021*, 1–40. https://doi.org/10.5194/wcd-3-337-2022

Rodgers, K. B., Lee, S. S., Rosenbloom, N., Timmermann, A., Danabasoglu, G., Deser, C., et al. (2021). Ubiquity of human-induced changes in climate variability. *Earth System Dynamics*, *12*(4), 1393–1411. https://doi.org/10.5194/esd-12-1393-2021

Simmonds, I., & Murray, R. (1991). A numerical scheme for tracking cyclone centres from digital data, part 1. *Australian Meteorological Magazine*, *39*, 155–166.

Sinclair, V. A., Rantanen, M., Haapanala, P., Räisänen, J., & Järvinen, H. (2020). The characteristics and structure of extra-tropical cyclones in a warmer climate. *Weather and Climate Dynamics*, *1*(1), 1–25. https://doi.org/10.5194/wcd-1-1-2020

Skamarock, W. C., Klemp, J. B., Duda, M. G., Fowler, L. D., Park, S. H., & Ringler, T. D. (2012). A multiscale nonhydrostatic atmospheric model using centroidal Voronoi tesselations and C-grid staggering. *Monthly Weather Review*, *140*(9), 3090–3105. https://doi.org/10.1175/mwr-d-11-00215.1

Skamarock, W. C., Park, S. H., Klemp, J. B., & Snyder, C. (2014). Atmospheric kinetic energy spectra from global high-resolution nonhydrostatic simulations. *Journal of the Atmospheric Sciences*, *71*(11), 4369–4381. https://doi.org/10.1175/jas-d-14-0114.1

Thompson, G., Field, P. R., Rasmussen, R. M., & Hall, W. D. (2008). Explicit forecasts of winter precipitation using an improved bulk microphysics scheme. Part II: Implementation of a new snow parameterization. *Monthly Weather Review*, *136*(12), 5095–5115. https://doi.org/10.1175/2008mwr2387.1

Ullrich, P. A., & Zarzycki, C. M. (2017). TempestExtremes: A framework for scale-insensitive pointwise feature tracking on unstructured grids. *Geoscientific Model Development*, *10*(3), 1069–1090. https://doi.org/10.5194/gmd-10-1069-2017

Ullrich, P. A., Zarzycki, C. M., McClenny, E. E., Pinheiro, M. C., Stansfield, A. M., & Reed, K. A. (2021). TempestExtremes v2. 1: A community framework for feature detection, tracking, and analysis in large datasets. *Geoscientific Model Development*, *14*(8), 5023–5048. https://doi.org/10.5194/gmd-14-5023-2021